Molecular Cell, Vol. 20, 313–324, October 28, 2005, Copyright ©2005 by Elsevier Inc. DOI 10.1016/j.molcel.2005.08.036

An Electrostatic Steering Mechanism of Cdc42 Recognition by Wiskott-Aldrich Syndrome Proteins

Lars Hemsath,[1] Radovan Dvorsky,[1] Dennis Fiegen,[1] Marie-France Carlier,[2] and Mohammad Reza Ahmadian[1,*]
[1]Abteilung Strukturelle Biologie
Max-Planck-Institut für Molekulare Physiologie
Otto-Hahn-Strasse 11
44227 Dortmund
Germany
[2]Dynamique du Cytosquelette
Laboratoire d'Enzymologie et Biochimie Structurale
CNRS 91198 Gif-sur-Yvette
France

Summary

The specific and rapid formation of protein complexes is essential for diverse cellular processes such as remodeling of actin filaments in response to the interaction between Rho GTPases and the Wiskott-Aldrich syndrome proteins (WASp and N-WASp). Although Cdc42, TC10, and other members of the Rho family have been implicated in binding to and activating the WAS proteins, the exact nature of such a protein-protein recognition process has remained obscure. Here, we describe a mechanism that ensures rapid and selective long-range Cdc42-WASp recognition. The crystal structure of TC10, together with mutational and bioinformatic analyses, proved that the basic region of WASp and two unique glutamates in Cdc42 generate favorable electrostatic steering forces that control the accelerated WASp-Cdc42 association reaction. This process is a prerequisite for WASp activation and a critical step in temporal regulation and integration of WASp-mediated cellular responses.

Introduction

The hematopoietic Wiskott-Aldrich syndrome protein (WASp) (Derry et al., 1994) and its ubiquitous homolog N-WASp (Miki et al., 1996) link intracellular signaling processes to the rearrangement of actin filaments. The generation of new actin filaments by branching is mediated by association of the Arp2/3 complex with WASp (Badour et al., 2003; Bompard and Caron, 2004; Higgs and Pollard, 1999; Millard et al., 2004; Miki and Takenawa, 2003; Takenawa and Miki, 2001; Thrasher, 2002). The C-terminal *v*erprolin homology, *c*entral and *a*cidic (VCA) region, also known as WCA or WA domain of the WAS proteins, binds the Arp2/3 complex as well as globular actin and thereby activates actin polymerization (Buck et al., 2001; Devriendt et al., 2001; Kim et al., 2000; Prehoda et al., 2000; Rohatgi et al., 1999). Besides this downstream activation domain, WASp consists of a central proline-rich domain, an N-terminal WASp homology 1 domain (WH1), and a G protein binding domain (GBD) encompassing a basic region (BR) and a Cdc42- and Rac1- interactive binding (CRIB) motif. In resting cells, WASp is in an autoinhibited state that is characterized by intramolecular interactions between its GBD and the VCA domain (Rohatgi et al., 1999). Binding of active Cdc42 to the GBD has been proposed to release the VCA domain from its masked conformation that is then able to activate the Arp2/3 complex (Buck et al., 2001, 2004; Kim et al., 2000; Miki et al., 1998).

Besides Cdc42, several other members of the Rho family have been reported to directly interact with N-WASp. These include Rac1, TC10, TCL, and RhoT, the latter being a mouse homolog of human TCL (Abe et al., 2003; Aspenstrom et al., 1995, 2004; Neudauer et al., 1998; Vignal et al., 2000). Some of these interactions, however, could not be observed in other reports (Miki et al., 1998; Symons et al., 1996). Therefore, we investigated the binding properties and specificity of the different GTPases regarding WASp and N-WASp association and activation.

Results

Kinetics of the Interaction between Cdc42 and the WAS Proteins

The GBDs of WASp and N-WASp share a high sequence identity (56% identity and 74% similarity) and exhibit similar activities in different qualitative assays. To gain insight into individual rate constants for the interaction of Cdc42 with both $WASp_{154–321}$ (WASpGBD) and $N\text{-}WASp_{142–276}$ (N-WASpGBD), a detailed kinetic analysis has been performed that takes advantage of fluorescence spectroscopy and mantGppNHp, a fluorescently labeled, nonhydrolyzable GTP analog. Figures 1A and 1B show that there is a rapid decrease of fluorescence upon mixing Cdc42·mantGppNHp with both GBDs in the stopped-flow apparatus. This represents the rapid-association process, as increasing concentrations of WASpGBD result in an incremental increase in the rate of the fluorescence change. The observed rate constants (k_{obs}) obtained by a single exponential fitting increase in a linear fashion as a function of the WASpGBD and N-WASpGBD concentrations (Figure 1C), yielding very high but similar association rate constants (k_{on}; Table 1). A possible intermediate encounter complex in the association reaction between Cdc42 and WASp, as shown for Ras-effector interactions (Kiel et al., 2004), could not be shown by the setup used above. Thus, we analyzed the association reactions at 10°C because the k_{obs} of the reactions at higher WASpGBD concentrations were too fast at 25°C and exceeded the constraints of the stopped-flow apparatus. As shown in Figure 1D, the hyperbolic dependency of the observed rate constants versus the WASp concentration strongly suggests that the Cdc42-WASp association follows a two-step reaction mechanism.

The dissociation of the GBDs from Cdc42·mantGppNHp was measured in a displacement experiment. Thus, an excess amount of the nonfluorescent Cdc42·GppNHp

*Correspondence: reza.ahmadian@mpi-dortmund.mpg.de

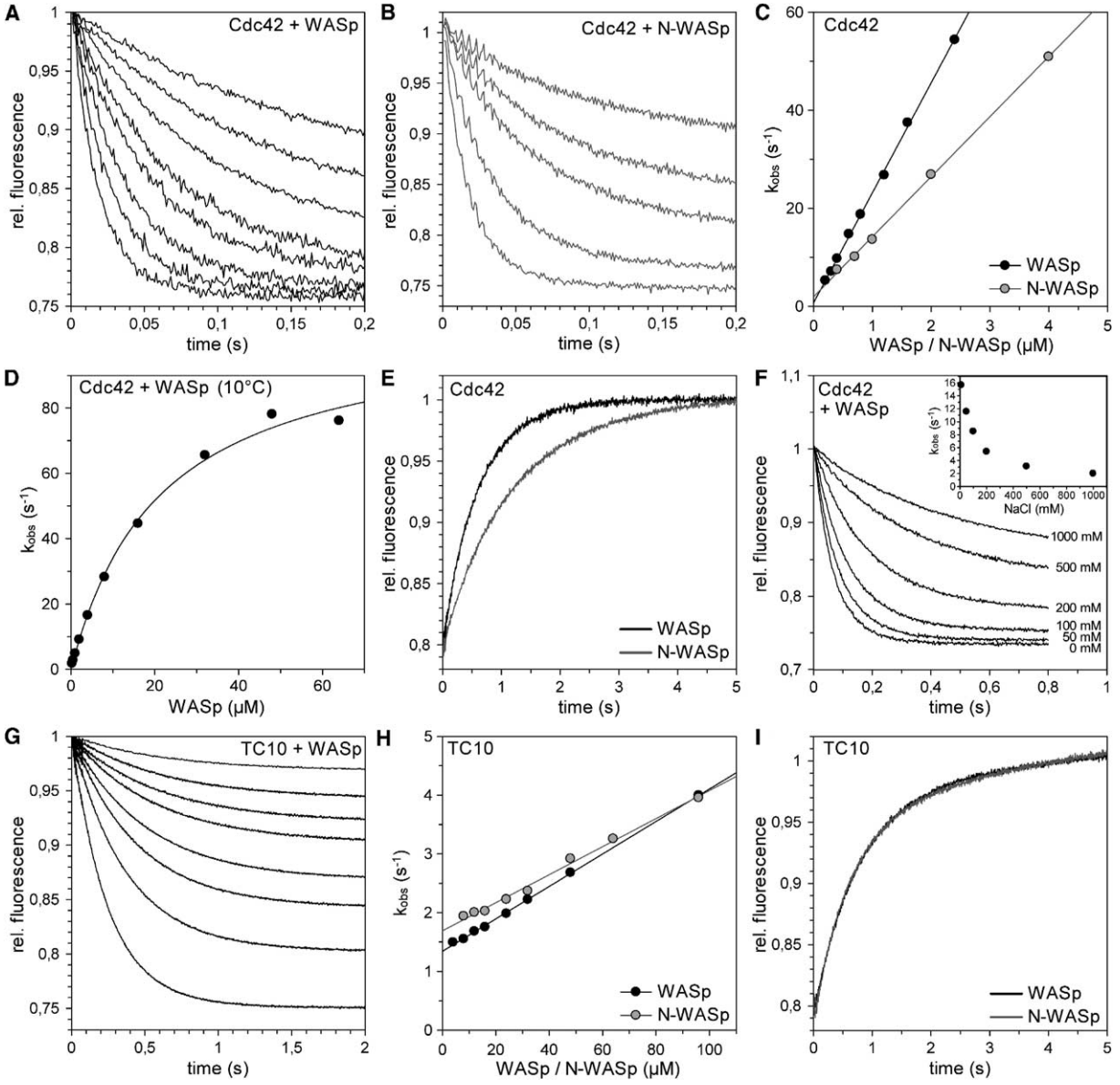

Figure 1. Kinetic Measurements of the Cdc42 Interaction with WASp and N-WASp

(A) Association of Cdc42·mantGppNHp (0.05 μM) with increasing WASpGBD concentrations (0.2–4 μM).
(B) Association of Cdc42·mantGppNHp (0.05 μM) with increasing N-WASpGBD concentrations (0.2–4 μM).
(C) Kinetics of the association between Cdc42 and the GBDs of the WAS proteins.
(D) Kinetics of the association between Cdc42 and the GBDs of the WAS proteins at 10°C (instead of 25°C as all other measurements).
(E) Dissociation of WASpGBD and N-WASpGBD from Cdc42·mantGppNHp (0.05 μM) in the presence of unlabeled Cdc42·GppNHp (5 μM).
(F) Association of Cdc42·mantGppNHp (0.1 μM) and WASpGBD (0.5 μM) in the presence of increasing NaCl concentrations (0–1000 mM). The k_{obs} values were plotted against the salt concentration (inset).
(G) Association of TC10·mantGppNHp (1.0 μM) with increasing WASpGBD concentrations (5–95 μM).
(H) Kinetics of TC10 association with the GBD of the WAS proteins.
(I) Dissociation of WASpGBD and N-WASpGBD from TC10·mantGppNHp (1.0 μM) in the presence of unlabeled Cdc42·GppNHp (100 μM).

was rapidly mixed with the protein complexes that led to a single exponential fluorescence increase (Figure 1E) and to similar values of dissociation rate constants for the two GBDs (k_{off}; Table 1). From the ratio of the dissociation and association rate constants ($K_d = k_{off} / k_{on}$), equilibrium dissociation constants (K_d) of 74 and 68 nM have been calculated for the Cdc42 interaction with WASpGBD and N-WASpGBD, respectively (Table 1). These high affinities are in good agreement with the values reported for the interaction of Cdc42 with shorter WASp fragments (Rudolph et al., 1998; Owen et al., 2000; Buck et al., 2004) and with the results of an alternative quantitative binding assay, the guanine nucleotide dissociation inhibition (GDI) assay (Table 1; see Figure S1 in the Supplemental Data available with this article online). It is important to note that we did not

Table 1. Kinetic Data of the Interaction of Different Rho GTPases with WAS Proteins and PAK1

	WASpGBD			N-WASpGBD			PAK1GBD		
	k_{on}	k_{off}	K_d	k_{on}	k_{off}	K_d	k_{on}	k_{off}	K_d
$Cdc42_{wt}$	22	1.7	0.074	12	0.84	0.068	0.61	0.096	0.16
$Cdc42_{wt}$			0.035[a]			0.051[a]			
$Cdc42_{K}$	3.5	3.3	0.95	2.2	1.9	0.90	0.31	0.090	0.29
$Cdc42_{KK}$	0.59	4.1	6.9	0.29	2.4	8.3	0.12	0.084	0.72
$TC10_{wt}$	0.028	1.2	43	0.024	1.7	70	0.012	0.056	4.7
$TC10_{E}$	0.18	1.0	5.8	0.21	1.2	5.9	nd	nd	nd
$TC10_{EE}$	0.22	0.83	3.7	0.38	1.1	2.8	nd	nd	nd
$TC10_{ITT}$	0.045	3.9	86	nd	nd	nd	nd	nd	nd
TCL_{wt}	no binding			no binding			0.005	0.065	15
$Rac1_{wt}$	no binding			no binding					0.49[a,b]
$Rac1_{E}$	no binding			no binding			nd	nd	nd
RhoA	no binding			no binding			no binding		

Association rates (k_{on} in $\mu M^{-1}s^{-1}$), dissociation rates (k_{off} in s^{-1}), and equilibrium dissociation constants (K_d in μM) of WASp, N-WASp, and PAK1 binding to the active mantGppNHp bound forms of different GTPases are summarized. K_d values have been calculated from the association and the dissociation rate constants ($K_d = k_{off}/k_{on}$). GTPases are as follows: $Cdc42_{K}$, Cdc42 E49K mutant; $Cdc42_{KK}$, Cdc42 E49K and E178K mutant; $TC10_{E}$, TC10 K63E mutant; $TC10_{EE}$, TC10 K63E and T192E mutant; $TC10_{ITT}$, TC10 M35I, A38T, and N39T mutant; $Rac1_{E}$, Rac1 K49E mutant; nd, not determined.

[a] Reference data determined by GDI assay (see Supplemental Data).

[b] Data by Fiegen et al. (2004).

observe a signal for binding of WASp to the inactive mantGDP bound form of Cdc42 (Figure S2).

Interaction of Other Rho GTPases with WASp or N-WASp

Other members of the Rho family, such as Rac1, TC10, TCL, and RhoT have been reported to directly interact with N-WASp (Abe et al., 2003; Aspenstrom et al., 1995, 2004; Neudauer et al., 1998; Vignal et al., 2000). Moreover, another study has shown that N-WASp, but not WASp, interacts with a constitutively active mutant of TC10, as observed with the yeast two-hybrid system (Neudauer et al., 1998). To shed light on this issue, both the GDI assay and kinetic measurements were performed with TC10. Under the conditions used for Cdc42, neither a GDI effect nor a fluorescence change of TC10·mantGppNHp could be detected by using WASpGBD or N-WASpGBD (data not shown). However, with 20-fold higher concentrations of TC10·mantGppNHp (1 μM), we succeeded in monitoring the association, which was incrementally accelerated in rate by increasing amounts of WASpGBD (Figure 1G). Similar data have been obtained for the association of N-WASpGBD (data not shown). The k_{on} values for the association of both GBDs with TC10, calculated from the linear regression plots (Figure 1H), are equal for WASp and N-WASp but, interestingly, are nearly three orders of magnitude lower than those with Cdc42 (Table 1).

In the plot of the k_{obs} values against the WASp/N-WASp concentration, there is a clear intercept on the y axis (Figure 1H), and this should correspond to the k_{off} values of 1.2 and 1.7 s^{-1}, respectively. These were measured in displacement experiments, which were carried out under the same conditions as described above for Cdc42 but with higher amounts of the respective components (Figure 1I). The results were in excellent agreement with the values obtained from the association experiments. Most remarkably, the determined k_{off} values for the WASp and N-WASp dissociation from TC10 are in the same range as those obtained for Cdc42 (Table 1). Thus, the binding constants for the interactions of TC10 with the WAS proteins obtained from the kinetic constants are up to 1000-fold higher than the respective data measured for Cdc42, which can be exclusively attributed to the association reactions.

Studies similar to those described for Cdc42 and TC10 were performed with TCL, the Rac isoforms (Rac1, Rac2, and Rac3) and RhoA at various GTPase concentrations, but they showed neither a direct fluorescence change nor a GDI effect upon addition of WASpGBD or N-WASpGBD (Figure S2), although these GTPases, with the exception of RhoA, do bind PAK1-GBD (residues 57–141) (Table 1). Thus, unlike PAK1, which binds to essentially all Rac/Cdc42-like GTPases, WAS proteins interact most specifically with Cdc42.

Salt-Dependency of the Cdc42-WASp Association

Kinetic data determined for the interaction of WAS proteins with Cdc42 and TC10 revealed the interactions to be exclusively association-controlled (Table 1). This strongly suggests that electrostatics may play a major role in the Cdc42-WASp recognition and complex formation. To examine this issue, we analyzed the relationship between k_{on} and ionic strength in the stopped-flow apparatus. As shown in Figure 1F, the observed rate constants for the WASp association with Cdc42·mantGppNHp incrementally dropped off in the presence of increasing salt concentrations, whereas the dissociation rates were not significantly changed (data not shown). High concentrations of salt counter ions obviously inhibit the attraction between Cdc42 and WASp, which clearly supports the idea that electrostatics are the driving forces for the extremely fast Cdc42-WASp association.

Identification of Hotspots for the Cdc42-WASp Association

To obtain structural information on TC10 and to explore the reason for the dramatic difference in WASp binding affinity between Cdc42 and TC10, we determined the crystal structure of the C-terminally truncated TC10·

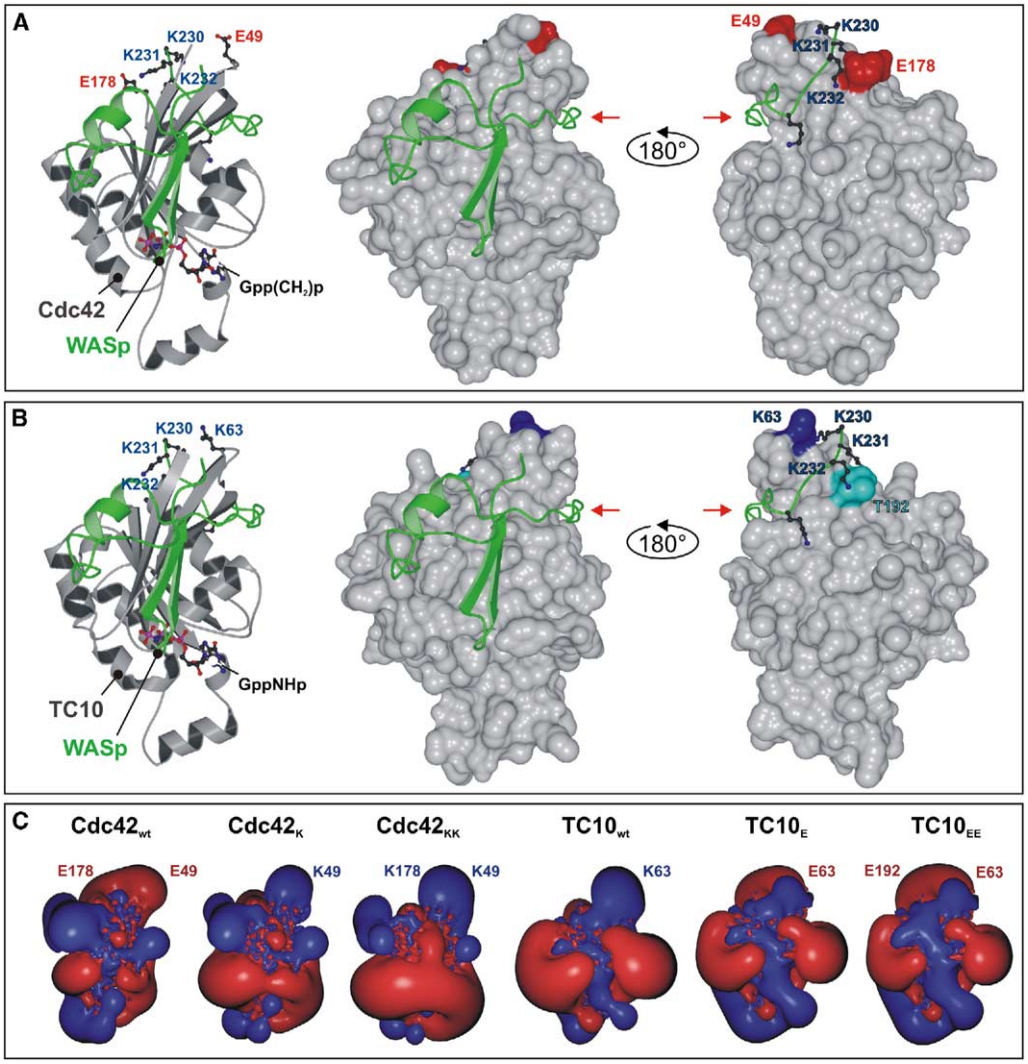

Figure 2. Specificity-Determining Residues in the GTPase-Effector Contact Sites

(A) Cdc42·Gpp(CH$_2$)p·WASpGBD complex according to Abdul-Manan et al., 1999. The ribbons (left) and the molecular surfaces (middle) of the structure are both illustrated in the same orientation. The third image (right) is rotated about the vertical axis by 180°. Cdc42 is gray, and WASpGBD is green. The indicated residues and the nucleotides are shown as ball and sticks. Red arrows point to the CRIB binding groove. The positions of the critical glutamates of Cdc42 and the lysines of WASpGBD are depicted in red and blue, respectively.

(B) The TC10·GppNHp·WASpGBD complex was modeled on the basis of the TC10·GppNHp structure (Table S1). The orientation of the structure and the illustration is according to (A). Lys63 and Thr192 of TC10 are shown in blue and cyan.

(C) Electrostatic potentials of wild-type and mutant forms of Cdc42 and TC10 are represented by their isosurfaces at –0.1 k_bT/e_c (red) or +0.1 k_bT/e_c (blue), respectively. The orientation of the molecules is the same as in (A) and (B) (left and middle). Residues critical for the association with WAS proteins, Glu49 (Lys63 in TC10), and Glu178 (Thr192 in TC10) of Cdc42 are indicated for orientation. Note that Glu178 and Thr192 are in fact on the other side of the proteins.

GppNHp complex at 2.65 Å resolution (Table S1). With respect to the WASp binding, the TC10 structure, interestingly, did not reveal any obviously significant three-dimensional deviations when compared to the Cdc42 structure in complex with WASp (Abdul-Manan et al., 1999) (Figures 2A and 2B). We next constructed a model of the TC10-WASp complex by superposition of TC10 on the Cdc42 structure in complex with WASp, which was finally refined by a few steps of energy minimization. As shown in Figures 2A and 2B, the overall structure of the model nicely resembles the Cdc42-WASp complex with the CRIB motif of WASp accommodated in the existing groove between α1, α5, and β2 on the surface of TC10. It is of interest to note that we failed to model the corresponding complex with RhoA and Rac1 using the RhoA·GTPγS (Ihara et al., 1998) and Rac1·GTP·p67^{Phox} (Lapouge et al., 2000) structures, which is probably attributable to the absence of such a groove in the RhoA and Rac1 structures.

In contrast to the kinetic data, no major differences between Cdc42 and TC10 could be detected when the primary sequence of both GTPases were compared, in particular concerning the residues involved in WASp binding according to the complex structure (Abdul-

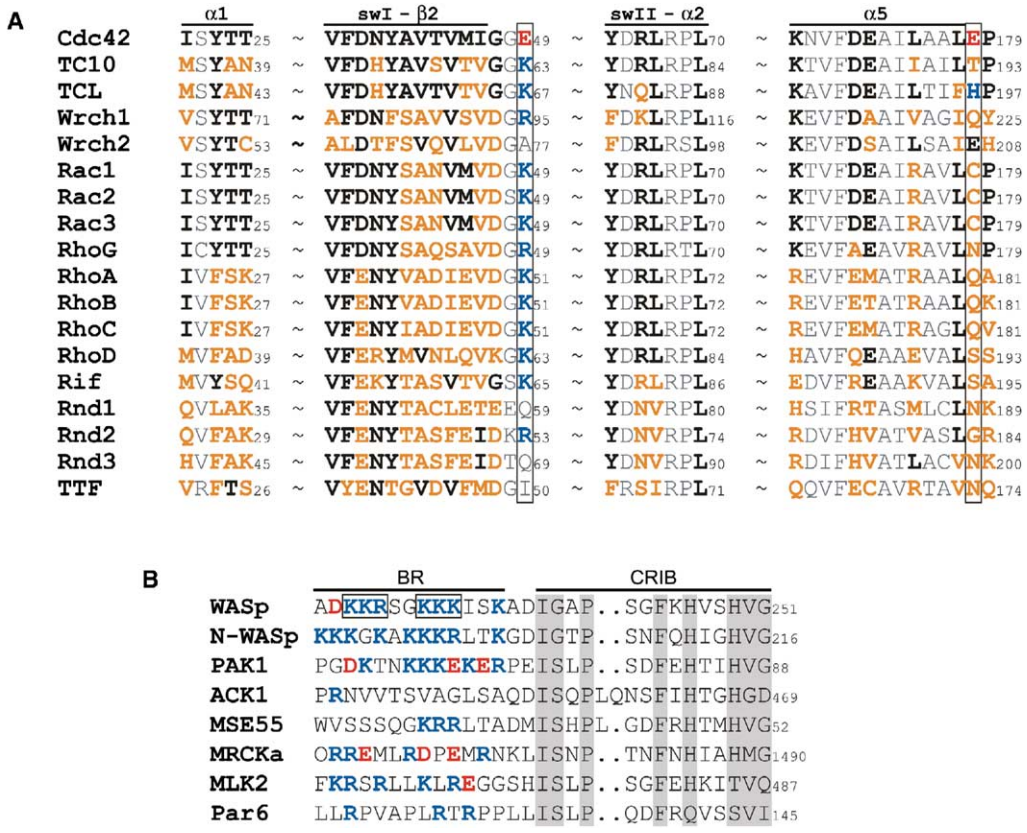

Figure 3. Amino Acid Sequence Alignments of Rho GTPases and CRIB-Containing Effectors

(A) Amino acid sequences of human Rho GTPases are aligned with respect to the WASp binding residues of Cdc42 according to Abdul-Manan et al., 1999. Conserved residues are black, variable residues are orange, and residues that do not contact WASp are gray. Glu49 and Glu178 of Cdc42 are red, and the corresponding residues in the other GTPases (boxed) are blue if positively charged. Secondary structure elements and motifs are highlighted at the top.

(B) Sequence comparison of CRIB-containing effectors. Positive (blue) and negative (red) residues of the basic region (BR) and conserved residues of the CRIB motif (gray background) are highlighted. The residues that were subjected to mutational studies are boxed.

Manan et al., 1999) (Figure 3A). Ile21, Thr24, and Thr25 of Cdc42 show minor deviations forming hydrophobic interactions with Phe244 of the CRIB motif of WASp. The corresponding residues in TC10 are Met35, Ala38, and Asn39, respectively. Substitution of these residues to the equivalent Cdc42 residues (referred to as $TC10_{ITT}$), however, did not increase the affinity of TC10 toward WASp or N-WASp, as characterized by kinetic measurements (Table 1). These data exclude a role of these three CRIB binding residues in determining the specificity toward the WAS proteins.

In addition to the binding residues, clusters of complementarily charged residues located in the vicinity of the protein-protein interfaces are often important for specific and efficient complex formation, as experimental and theoretical studies have demonstrated (Schreiber, 2002). Electrostatic steering, accomplished by such residues, has been shown to enhance the association rate (Kiel et al., 2004; Sheinerman et al., 2000; Sinha and Smith-Gill, 2002). Thus, we examined charged residues in the GTPases beyond the WASp binding regions because of the following: (1) the association reaction represents the main difference between Cdc42 and TC10 in their interaction with the WAS proteins (Table 1); (2) the WASp binding interface is conserved for both GTPases (Figures 2A and 3A); (3) the Cdc42-WASp association follows a two-step reaction mechanism with the first step being the formation of an encounter complex, which evolves into the final complex (Figure 1D); and (4) high salt concentration interferes with the Cdc42-WASp association (Figure 1F). A conspicuous amino acid deviation in Cdc42 is the unique Glu49. This residue is located on the solvent-exposed surface of the loop between the β strands 2 and 3 (Figure 2A) and corresponds to lysine or arginine in most other Rho GTPases (Figure 3A). According to the structure of the Cdc42 and WASp complex (Abdul-Manan et al., 1999), this glutamate does not directly interact with WASp but lies in the vicinity of three lysines of WASp (KKK motif; residues 230–232), which is part of the BR (residues 225–235). Glu178 of Cdc42, which is also absent in nearly all Rho GTPases (Figure 3A), provides another negative charge that is also in close vicinity of the KKK motif of WASp (Figures 2A and 3B).

Mutational Analysis of the GTPase-WASp Interaction

To examine the significance of these two glutamates in the interaction between Cdc42 and WASp, we gener-

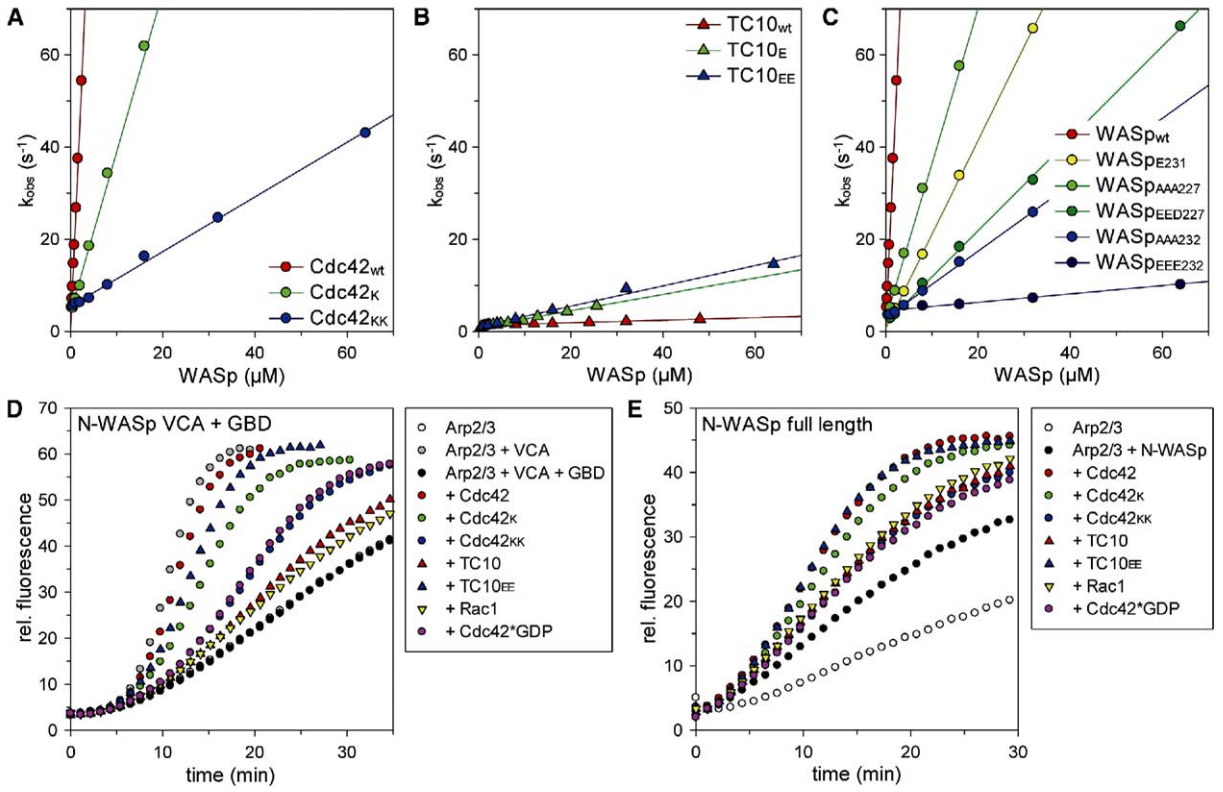

Figure 4. Mutational Analyses of Cdc42, TC10, and WASpGBD

(A) Kinetics of WASpGBD association with Cdc42 wild-type and mutants.
(B) Kinetics of WASpGBD association with TC10 wild-type and mutants.
(C) Kinetics of Cdc42 association with WASpGBD wild-type and mutants.
(D) Polymerization of pyrene-labeled actin (2.5 μM) by the Arp2/3 complex (0.02 μM) was measured in the presence and absence of the isolated N-WASpGBD (1 μM), N-WASpVCA (0.1 μM), and various wild-type and mutant GTPases in GDP and GppNHp-bound forms (2 μM).
(E) Actin polymerization under the same conditions as in (D), using full-length N-WASp (0.1 μM) instead of isolated GBD and VCA domains.

ated a single mutant, E49K, and a double mutant, E49K/E178K, of Cdc42 (referred to as $Cdc42_K$ and $Cdc42_{KK}$). The association and dissociation kinetic constants (k_{on} and k_{off}) of the interaction of WASp and N-WASp with the purified Cdc42 mutants were determined under the same condition as described above for $Cdc42_{wt}$ (Figure 4A; Table 1). The resulting K_d values were 12-fold higher for $Cdc42_K$ (950 nM) and about 93-fold higher for $Cdc42_{KK}$ (6.9 μM). The individual rate constants clearly reveal that incremental loss of binding affinity of the WAS proteins for the Cdc42 mutants is merely caused by decreased association rates, whereas the dissociation rates are not affected (Table 1). It is important to note that the affinity of Cdc42 proteins toward the less specific effector PAK1 is nearly unchanged by the mutations (only 2-fold and 4.5-fold reduction, respectively).

The corresponding mutations in TC10 (K63E, referred to as $TC10_K$, and K63E/T192E, referred to as $TC10_{KK}$) provided K_d values of 5.8 μM and 3.7 μM, which correspond to affinity increases of 8- and 13-fold, respectively (Figure 4B). These data, as summarized in Table 1, demonstrate again that the association rate almost exclusively contributes to the change of the binding affinity. In contrast, substitution of lysine 49 of Rac1 (referred to as $Rac1_E$) to glutamate did not result in any measurable binding of WASp or N-WASp (Table 1).

The BR and the CRIB of the GBD have been suggested to cooperatively regulate activation of the WAS proteins through binding to phosphatidylinositol-4,5-bisphosphate (PIP2) and activated Cdc42, respectively (Prehoda et al., 2000; Miki et al., 1998; Symons et al., 1996; Higgs and Pollard, 2000; Rohatgi et al., 2000). Judging from the Cdc42-WASpGBD complex structure (Abdul-Manan et al., 1999), the abundance of positively charged residues in the BR of the WAS proteins, however, strongly suggests that they might serve as a counterpart to the two glutamates of Cdc42. To test this assumption, we substituted both the KKR and KKK motifs of WASpGBD (Figure 3B) for neutral or negatively charged residues (referred to as $WASpGBD_{AAA227}$, $WASpGBD_{EED227}$, $WASpGBD_{AAA232}$, and $WASpGBD_{EEE232}$), respectively, and Lys231 for a glutamate ($WASpGBD_{E231}$) and investigated the kinetics of the interaction of these proteins with $Cdc42_{wt}$. Unlike earlier work in which deletion of the BR did not affect binding of N-WASpGBD to Cdc42 (Rohatgi et al., 2000), our kinetic measurements revealed a significant impairment of the Cdc42-WASpGBD interaction capacity when we employed single or triple mutants instead of the $WASpGBD_{wt}$ (Table 2). In this regard, there is a

Table 2. Kinetic Data of the Interaction of Cdc42 with WASpGBD Mutants

	$Cdc42_{wt}$		
	k_{on}	k_{off}	K_d
$WASpGBD_{wt}$	22	1.7	0.074
$WASpGBD_{AAA227}$	3.4	1.4	0.41
$WASpGBD_{EED227}$	1.0	1.6	1.6
$WASpGBD_{AAA232}$	0.72	1.9	2.6
$WASpGBD_{EEE232}$	0.09	3.0	33
$WASpGBD_{E231}$	0.59	4.1	6.9

The binding constants of the interaction of $Cdc42_{wt}$ and different WASpGBD mutants are listed according to the data in Table 1. $WASpGBD_{AAA227}$: WASpGBD K225A, K226A, and R227A mutant; $WASpGBD_{EED227}$: WASpGBD K225E, K226E, and R227D mutant; $WASpGBD_{AAA232}$: WASpGBD K230A, K231A, and K232A mutant; $WASpGBD_{EEE232}$: WASpGBD K230E, K231E, and K232E mutant; $WASpGBD_{E231}$: WASpGBD K231E mutant.

clear difference concerning mutations of the KKR and KKK motifs on the one hand and a clear increase in K_d values when the net positive charges were decreased on the other hand (Figure 4C). The latter phenomenon is best demonstrated with the K231E mutation in the middle of the KKK motif that led to a drop by two orders of magnitude in WASpGBD affinity for Cdc42 (Table 2). Consequently, a dramatic loss of binding affinity (450-fold) was observed with the $WASpGBD_{EEE232}$ mutant. These data, together with the recurring observation in this study that only the association reaction is affected by point mutations, but not the dissociation reaction, per se, strongly suggest that the BR of WASp, particularly the KKK motif, provides the most critical residues to establish the electrostatic steering effect. The binding affinity of TC10 for the WASpGBD mutants was only slightly affected (data not shown), further indicating that the TC10-WASp association does not underlie an electrostatic steering mechanism.

WASp acts as a scaffold for binding the actin nucleating Arp2/3 complex and triggers actin polymerization upon activation by Cdc42. Thus, it was important to prove our kinetic data concerning electrostatics in the Cdc42-WASp association by an alternative WASp-driven functional assay. Therefore, we performed in vitro actin polymerization experiments using purified proteins such as full-length N-WASp or N-WASp domains (GBD, VCA) and pyrene-labeled actin as described previously (Prehoda et al., 2000; Rohatgi et al., 1999, 2000; Higgs and Pollard, 2000; Carlier et al., 2000; Peterson et al., 2004; Torres and Rosen, 2003). As shown in Figure 4D, the function of the isolated VCA domain of N-WASp as a potent activator of the Arp2/3 complex in the pyrene-actin polymerization assay was completely inhibited when a 10-fold excess of N-WASpGBD was added to the reaction. According to our kinetic data described above and other studies (Prehoda et al., 2000; Higgs and Pollard, 2000; Rohatgi et al., 2000), wild-type Cdc42·GppNHp, but not its mutants ($Cdc42_K$ and $Cdc42_{KK}$), most efficiently accelerated the actin polymerization by displacing the VCA from its complex with the GBD (Figure 4D). In contrast, the activities of GppNHp bound TC10 and Rac1 were almost comparable to the basal level of the Arp2/3 complex-mediated actin polymerization (Figure 4D). Interestingly, substitution of glutamates 49 and 178 to lysines in Cdc42 strongly affected the actin polymerization rate, comparable to the effect of the inactive Cdc42·GDP. On the contrary, $TC10_{EE}$ was able to activate the reaction almost up to the level of $Cdc42_{wt}$ (Figure 4D). Moreover, it is important to note that similar data were obtained with full-length N-WASp instead of the isolated GBD and VCA domains of WASp (Figure 4E). Taken together, these data are in excellent agreement with our kinetic data on the WASp interaction with the GTPases and clearly support the conclusion that electrostatic steering forces are critical components for Cdc42-WASp signaling.

Electrostatic Potentials of Cdc42 and TC10

An important role of electrostatic interactions is the steering of two proteins when they approach each other. The interactions accelerate their proper orientation and increase the rate of their association. Therefore, we calculated the electrostatic potential of $Cdc42_{wt}$ (Figure 2C) and compared it with the electrostatic potentials of the respective Cdc42 mutants ($Cdc42_K$ and $Cdc42_{KK}$). The "lobe" of negative potential around Cdc42 significantly decreases, particularly in the region where WASp positions the KKK motif of its BR (Figure 2C). Accordingly, the electrostatic binding energy of –510 kcal/mol calculated from the NMR structure of the Cdc42-WASp complex (Abdul-Manan et al., 1999) according to the Poisson-Boltzmann equation (see Experimental Procedures) was increased to –457 kcal/mol and –277 kcal/mol in $Cdc42_K$ and $Cdc42_{KK}$, respectively. It is of interest to note that the negative potentials of $Cdc42_{wt}$ in the vicinity of the BR of WASp were almost replaced by a positive electrostatic potential when Glu49 of Cdc42 was substituted by a lysine. This scenario is in good agreement with the findings of electrostatic potential calculations for TC10 as demonstrated by the equipotential contours of $TC10_{wt}$ (Figure 2C) versus $TC10_E$ and, thus, nicely explains the dramatic difference of the k_{on} values for the WASpGBD association with Cdc42 and TC10 (Table 1). As a consequence, TC10 mutation at Lys63 and Thr192 to glutamates resulted in a drastic increase in electrostatic binding energies.

Discussion

Over the past few years, Rho GTPase interactions with their effector domains were well investigated both by biochemical and structural means (Bishop and Hall, 2000; Dvorsky and Ahmadian, 2004). This, however, has only in a few cases shed light on the mechanism of effector activation, which in most cases requires the disruption of intramolecular autoinhibition and the exposure of functional domains. One exception constitutes the interaction of WASp and N-WASp with Cdc42. This effector family has been extensively studied by several groups, resulting in a better understanding of how these regulatory mechanisms are integrated to control the localized activation of Arp2/3 (Prehoda et al., 2000; Rohatgi et al., 1999, 2000; Higgs and Pollard, 2000; Carlier et al., 2000; Yang et al., 2000). Biochemical and

NMR spectroscopic studies revealed mechanistic and structural details of the regulation of WASp and N-WASp, including its activation by Cdc42 through an allosteric mechanism (Buck et al., 2001, 2004; Kim et al., 2000; Abdul-Manan et al., 1999; Torres and Rosen, 2003; Cory et al., 2003). An important yet open issue, however, is the molecular mechanism of Cdc42 recognition by the WAS proteins, which is a critical step in regulating and integrating WASp signaling over time. Thus, this study investigated the interaction of the WAS proteins with different Rho GTPases in detail using biochemical, structural, and computational methods. Our results provide strong evidence for electrostatic steering as the primary and initial mechanism of molecular recognition of Cdc42·GTP by WASp and N-WASp.

With the presented data, we clearly show that the signal transduction of Cdc42 through WASp is association controlled. This is nicely documented by a nearly identical k_{off} and three orders of magnitude difference in the k_{on} value for the interaction of the WASpGBDs with Cdc42 versus TC10 (Table 1). Unlike earlier qualitative binding studies (Abe et al., 2003; Aspenstrom et al., 1995, 2004; Neudauer et al., 1998; Vignal et al., 2000), however, we did not detect any interaction of WASp or N-WASp with Rac1 and TCL even at high GBD concentrations of up to 50 μM and using two different fluorescence spectroscopic methods (Figure S2). The main reason for this is the two glutamates Glu49 and Glu178 of Cdc42, which are replaced by positively charged residues at the corresponding positions in most other Rho GTPases (Figure 3A). It is important to note that these residues are not part of the switch regions and thus are not involved in the nucleotide-dependent structural change of Cdc42 (Dvorsky and Ahmadian, 2004).

The electrostatic potential of the GppNHp bound structures of Cdc42 and TC10 allows the visualization of the opposed electrostatics of these GTPases (Figure 2C), which, when mutated, led to a loss of function in the case of Cdc42 and gain of function in the case of TC10. Experimental evidence has shown that electrostatics substantially enhance the association rate in a number of systems and thus play a major role in defining the mechanisms of molecular recognition and complex formation (Schreiber, 2002; Kiel et al., 2004; Sheinerman et al., 2000; Sinha and Smith-Gill, 2002). Recently, it has been shown that the generation of structurally based mutants in the Ras binding domain of an effector results in its faster binding to Ras (up to 25-fold due to an optimal electrostatic steering; Kiel et al., 2004). A double substitution of both glutamates 49 and 178 by lysines ($Cdc42_{KK}$) resulted in a 122-fold reduction of binding affinity. More noteworthy, however, is the fact that only the association rates of the mutants are affected, but not the dissociation rates (Table 1), emphasizing these residues as the hotspots for association. These kinetic data are supported by a functional assay that utilizes the scaffolding function of the WAS proteins in activating the Arp2/3 complex toward actin polymerization only in response to active $Cdc42_{wt}$ (Figures 4D and 4E). Our observations strongly suggest that a fine-tuning of local and global electrostatic properties, in particular Glu49, is essential for the molecular recognition of Cdc42 by WAS proteins and further substantiates the significance of long-range charge-charge interactions in defining the mechanism of association, which is naturally absent in TC10.

On the other hand, our structural and biochemical data indicate that the interacting interfaces of WASp with Cdc42 and TC10 in the final complex are comparable, as TC10 contains a conserved WASp binding site (Figures 2A and 2B) and has k_{off} values in the same range as Cdc42 (Table 1). Amino acid deviations of the α1 helix of TC10 (CRIB binding region) were also proved not to contribute to the dramatic difference—three orders of magnitude—in k_{on} values (Table 1). Introduction of negative charges in TC10 ($TC10_{E/EE}$) most interestingly led to a reasonably faster association with the WAS proteins, but it does not reach the rate of the Cdc42-WASp association. In this regard, calculated electrostatic potentials of the wild-type and mutant Cdc42 and TC10 provided striking insights (Figure 2C). In Cdc42, the "lobe" of negative potential (e.g., Glu49 and Glu178) is surrounded by the positive potential of several basic residues (e.g., His103, His104, Lys107, Lys150, and Lys153), which most likely help to direct the optimal orientation of Cdc42 to WAS proteins. This cannot be accomplished in TC10, which lacks these surrounding positively charged residues and, rather, exhibits an extended negative potential close to the association-determining residues. This data and the fact that the substitution of both glutamates in Cdc42 ($Cdc42_{KK}$) did not reduce its association rate to the same level as determined for $TC10_{wt}$ (Table 1) indicate that other structural features apart from the two glutamates also contribute to the Cdc42-WASp association.

Thus, an electrostatic steering mechanism seems unlikely in the case of TC10 given the observation that changes of the net charge within the BR of WASp have only a minor effect on TC10 binding. In particular, we did not observe any significant TC10-mediated displacement of the VCA domain in the actin polymerization assay (Figures 4D and 4E). It seems that TC10, which lacks such a negative patch, is disabled in recognizing and disrupting the autoinhibited state of the full-length WASp. In conclusion, understanding the role of TC10 in activating WASp or N-WASp as possible downstream effectors, however, remains one of the more challenging tasks. We think that depending on the cellular context, the TC10·GTP·WASp complex formation requires assistance from an accessory factor (protein or lipids) that should help both molecules to overcome the 800-fold-slower association rate.

Nevertheless, by generating electrostatic forces for a more efficient TC10-WASp association by using the $TC10_{EE}$ mutant, we have enhanced the capability of TC10 in WASp activation up to the level of $Cdc42_{wt}$ (Figures 4D and 4E). This is remarkable because the k_{on} value for the association of $TC10_{EE}$ with the WAS proteins is still 100-fold below that measured for $Cdc42_{wt}$ (Figures 1C and 4B; Table 1). In contrast to the kinetic measurements, which determine bimolecular interactions, enhanced actin polymerization requires both the GTPase association with WASp and the release of the Arp2/3 activator VCA. In the autoinhibited conformation of WASp, the C-terminal part of the GBD is masked by the VCA domain, as shown by structural analysis (Kim et al., 2000). According to our model (Figure 5), initial binding of Cdc42 to the WASpBR is re-

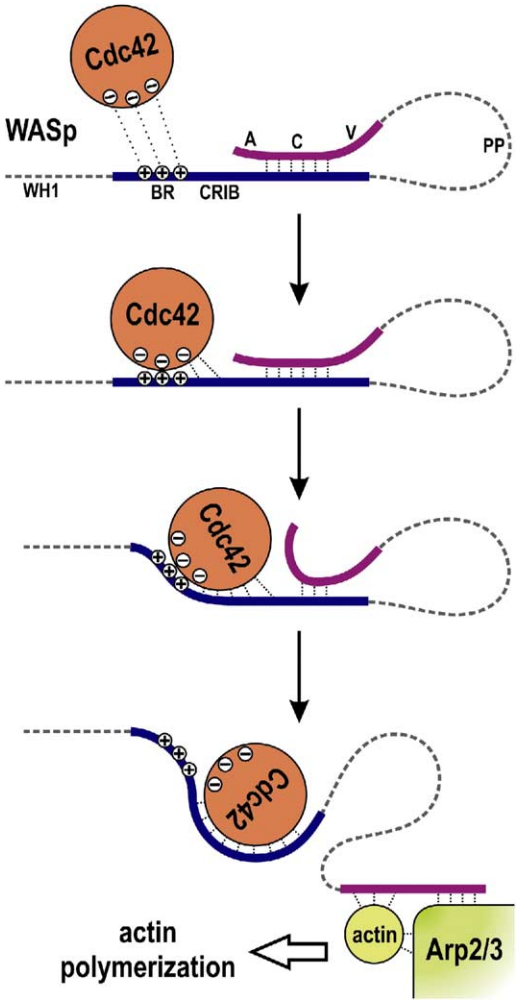

Figure 5. Model of the Electrostatic Steering Mechanism for the Association of the Autoinhibited WASp with Cdc42

The WASpGBD with the basic region (BR) and the CRIB motif is shown in blue and the C-terminal VCA peptide in magenta. The plus sign stands for positively charged residues and the minus sign indicates negatively charged residues. Abbreviations are as follows: WH1, WASp homology 1; PP, polyproline region.

quired for the VCA displacement. Although $TC10_{EE}$ cannot establish an effective electrostatic steering with WASp, in the actin polymerization assay it may form the required complex with the BR of WASp via the two inserted glutamates and, thus, facilitate the release of VCA even more than $Cdc42_{wt}$. $Cdc42_{KK}$, on the other hand, though having a comparable affinity towards WASp as $TC10_{EE}$ (Table 1), is not able to bind the BR because of the repulsive forces generated by the two positively charged regions.

WASpGBD binds to four different regions (α1, switch I/β2, switch II/α2, and α5) of Cdc42 (Abdul-Manan et al., 1999), which show striking amino-acid deviations at the equivalent positions in GTPases of the Rho family (Figure 3A). This might be the reason that compared to TC10, we did not observe any interaction of the WAS proteins with Rac1 and TCL/RhoT. The latter share higher identity with TC10 at these regions, but there are two additional deviations in TCL (Asn84 and Gln85 instead of Asp65 and Arg66, respectively, in Cdc42; and Phe195 and His196 instead of Leu177 and Glu178, respectively), which might be another reason for its lack of binding to WASp. Thus, we exclude WAS proteins as the downstream effectors for TCL and propose that it may target other effector molecules involved in filopodia formation (Passey et al., 2004).

The basic region of the WAS proteins has been proposed to be involved in PIP2 binding that in turn plays a part in the Cdc42-mediated regulation of WAS protein activity (Prehoda et al., 2000; Miki et al., 1998; Symons et al., 1996; Higgs and Pollard, 2000; Rohatgi et al., 2000). Kinetic measurements carried out by using point mutations within the WASpBR clearly revealed that positively charged residues (Figure 3B) of the BR strongly contribute to the association reaction of the Cdc42-WASp interaction. Any changes of the basic residues in this region, particularly those of the KKK-motif, caused a significant loss of binding affinity, which is again primarily attributed to the changes of the association reaction (Figure 4C; Table 2). Taken together, we propose that the BRs of the WAS proteins play a critical role in Cdc42 recognition by supplying complementary electrostatics to the two unique glutamates 49 and 178 and is therefore in addition to the CRIB motif an integral component of the WASp and N-WASp GBD. It is important to note that in this regard we could not detect any interdependency between Cdc42 and PIP2 in WASp binding and activation (Figure S3).

An electrostatic steering mechanism can be excluded for most of the other Cdc42 effectors, which do not contain, with a few exceptions, a characteristic BR (Figure 3B). PAK consists of a KKKEKER motif (with a net charge of 3) that is equivalent to the BR of the WASps, indicating that it may electrostatically assist the Cdc42-PAK association. Our data, however, exclude a major role of electrostatic steering for two reasons. First, the k_{on} value for the PAK association with Cdc42 (which is 40-fold lower compared to the WASp association) was not changed when the critical glutamates in Cdc42 were replaced by lysines (Table 1). Secondly, PAK binds Cdc42 and Rac1 with 3-fold lower affinities, although Rac1 contains a lysine and a cysteine instead of the two critical glutamates (Figure 3A; Table 1). An explanation for this fact may be that in the Cdc42-PAK complex, the two glutamates of PAK (Glu69 and Glu71; Figure 3B) are in the vicinity of Glu49 of Cdc42 (Gizachew et al., 2000) and thus counteract the formation of the encounter complex. These and other effectors such as ACK, MLK, MRCK, and Par6 therefore need to employ alternative mechanisms in order to compete with WAS proteins and to efficiently associate with Cdc42·GTP.

As expected from their identity in sequence and in cellular action (Badour et al., 2003; Bompard and Caron, 2004; Higgs and Pollard, 1999; Millard et al., 2004; Miki and Takenawa, 2003; Takenawa and Miki, 2001; Thrasher, 2002), both WASp and N-WASp behave nearly identically in their GTPase binding characteristics (Table 1), suggesting a common mechanism by which Cdc42 activates the WAS proteins to stimulate the Arp2/3-mediated actin polymerization. Based on

our kinetic studies and the available structural data (Kim et al., 2000; Abdul-Manan et al., 1999), we propose a model for an electrostatic steering mechanism, which, resulting from long-range charge-charge interactions, dictates selective recognition of Cdc42 by WAS proteins (Figure 5). In the autoinhibited state (Kim et al., 2000), the C-terminal VCA domain of WASp interacts with many of the residues of the GBD that are also involved in the Cdc42-WASp interaction (Abdul-Manan et al., 1999), except for the BR and the CRIB. Cdc42 first approaches these regions and initiates a cooperative binding process (Buck et al., 2001, 2004) that includes both destabilization of the secondary structure elements of the autoinhibited WASp and folding of the GBD (Abdul-Manan et al., 1999). The complex formation with Cdc42 acts in synergy with different other local signals including PIP2, SH3-containing proteins (e.g., Grb2, NCK), and phosphorylation (Benesch et al., 2002; Bompard and Caron, 2004; Buck et al., 2004; Carlier et al., 2000; Higgs and Pollard, 1999; Prehoda et al., 2000; Rohatgi et al., 1999, 2000; Suetsugu et al., 2002; Torres and Rosen, 2003), which coordinately facilitate the activation of the Arp2/3 complex toward actin polymerization.

Conclusion

Over the past few years, four major, partly overlapping levels of regulation of the activity of WASp proteins have been uncovered (Bompard and Caron, 2004): interaction with binding partners, degradation, phosphorylation (Torres and Rosen, 2003; Cory et al., 2003), and subcellular distribution. In the present study, we propose an association-controlled mechanism for the selective Cdc42 recognition by the WAS proteins. With the basic region in WASps and the two glutamates in Cdc42, we identified two hotspots, which control the long-range interaction between active Cdc42 and the inactive WAS protein. This phenomenon, called electrostatic steering, is a critical step in initiating the Cdc42-mediated activation of the WAS proteins and dictates integration and transmission of signals in time. By definition, the involved components need not be necessarily involved in the final complex formation. Cdc42 causes not only the release of VCA but also the exposure of BR for interaction with the plasma membrane messenger PIP2.

Experimental Procedures

Plasmids

Human Cdc42 (residues 1–178; accession number nm_001791), Rac1 (1–184; nm_006908), RhoA (1–181; L25080), TC10 (2–193; nm_012249), human WASpGBD (154–321; u19927), N-WASpGBD (142–276; nm_003941), and PAK1GBD (57–141; nm_002576) were cloned into pGEX expression vectors (pGEX 2T or pGEX 4T1). Mutations in Cdc42, Rac1, TC10, and WASp were obtained by QuikChange PCR mutagenesis (Stratagene).

Protein Preparation

All proteins were produced as glutathione S-transferase (GST) fusion proteins in *Escherichia coli* BL21 Rosetta. Glutathione (GSH-) sepharose (Pharmacia, Uppsala, Sweden) was used as the first purification step. After protease cleavage of the GST-tags, the proteins were applied to a gel filtration column (Superdex 75 or 200, Pharmacia, Uppsala, Sweden) and a subsequent GSH-sepharose column as the final step to obtain a purity of at least 95%. GppNHp- (guanosine 5′-β,γ-imidotriphosphate) and mantGppNHp (2′,3′-O-N-methylanthraniloyl-GppNHp) bound GTPase proteins were prepared by degrading bound GDP by alkaline phosphatase in the presence of 1.5-fold molar excess of GppNHp or mantGppNHp as described (Ahmadian et al., 2002). A prepacked gel filtration column (NAP5, Pharmacia) was used to remove unbound nucleotides. The concentrations of nucleotide bound proteins were determined by HPLC as described (Ahmadian et al., 2002). His-tagged N-WASp full-length was purified from High Five insect cells (Invitrogen) (Egile et al., 1999). The Arp2/3 complex was isolated from bovine brain (Egile et al., 1999), and actin was purified from rabbit muscle and labeled with pyrenyliodoacetamide (Pantaloni et al., 2000).

Fluorescence Measurements

Kinetic measurements of the GTPase-effector interaction were monitored with the fluorescently labeled GTP-analog mantGppNHp by using an excitation wavelength of 366 nm. The emission was detected at 450 nm or with a cut-off filter above 408 nm. Slow kinetics were monitored in a Perkin-Elmer fluorescence spectrometer (LS50B, Norwalk, CT), and fast kinetics were monitored in a stopped-flow apparatus (Applied Photophysics, SX18MV, Surrey, UK). All measurements were performed in 30 mM Tris-HCl (pH 7.5), 5 mM $MgCl_2$, 50 mM NaCl, and 3 mM DTT at 25°C. Data obtained by the stopped-flow apparatus are averages of at least four independent measurements. Kinetic measurements of the direct binding of an effector to a mantGppNHp bound GTPase were carried out using the stopped-flow apparatus. Dissociation experiments were performed by displacing the bound effector from the complex with the mantGppNHp bound GTPase with an excess of unlabeled GppNHp bound GTPase to prevent it from reassociation with the labeled GTPase. The observed rate constants were fitted single exponentially using the GraFit program (Erithacus software).

Actin Polymerization Assay

The actin polymerization assays were performed according to M.-F. Carlier (Carlier et al., 2000). Briefly, 20 nM Arp2/3 complex was mixed with 100 nM N-WASp (full-length) or 100 nM N-WASpVCA and 1 μM N-WASpGBD in 5 mM Tris-HCl (pH 7.6), 0.1 mM $CaCl_2$, 0.2 mM ATP, 1 mM dithiothreitol, 0.01% NaN_3 containing 100 mM KCl, 1 mM $MgCl_2$, and 0.2 mM EGTA. Accessorily, 2 μM GppNHp bound GTPase was added to test its activation ability. After addition of 2.5 μM actin (10% pyrene-labeled), the reaction was monitored in a Xenius fluorescence spectrometer (SAFAS, Monaco, France) with an excitation wavelength of 366 nm and an emission wavelength of 407 nm.

Supplemental Data

Supplemental Data including three figures, one table, Supplemental Results, Experimental Procedures, and References are available online with this article at http://www.molecule.org/cgi/content/full/20/2/313/DC1/.

Acknowledgments

We gratefully thank A. Wittinghofer for discussions and continuous support; P. Stege for excellent technical assistance; and R. Goody and C. Herrmann for critically reading the manuscript. This work was supported by the Volkswagen-Stiftung (L.H.) and a Marie Curie Fellowship of the European Community (R.D.) and by a scholarship of the Verband der Chemischen Industrie (D.F.). M.-F.C. acknowledges financial support from the Ligue Nationale Contre le Cancer and from the HFSP grant RGP0072/2003-C.

Received: April 21, 2005
Revised: August 2, 2005
Accepted: August 31, 2005
Published: October 27, 2005

References

Abdul-Manan, N., Aghazadeh, B., Liu, G.A., Majumdar, A., Ouerfelli, O., Siminovitch, K.A., and Rosen, M.K. (1999). Structure of Cdc42

in complex with the GTPase-binding domain of the 'Wiskott-Aldrich syndrome' protein. Nature *399*, 379–383.

Abe, T., Kato, M., Miki, H., Takenawa, T., and Endo, T. (2003). Small GTPase Tc10 and its homologue RhoT induce N-WASP-mediated long process formation and neurite outgrowth. J. Cell Sci. *116*, 155–168.

Ahmadian, M.R., Wittinghofer, A., and Herrmann, C. (2002). Fluorescence methods in the study of small GTP-binding proteins. Methods Mol. Biol. *189*, 45–63.

Aspenstrom, P., Fransson, A., and Saras, J. (2004). Rho GTPases have diverse effects on the organization of the actin filament system. Biochem. J. *377*, 327–337.

Aspenstrom, P., Lindberg, U., and Hall, A. (1995). Two GTPases, Cdc42 and Rac, bind directly to a protein implicated in the immunodeficiency disorder Wiskott-Aldrich syndrome. Curr. Biol. *6*, 70–75.

Badour, K., Zhang, J.Y., and Siminovitch, K.A. (2003). The Wiskott-Aldrich syndrome protein: forging the link between actin and cell activation. Immunol. Rev. *192*, 98–112.

Benesch, S., Lommel, S., Steffen, A., Stradal, T.E.B., Scaplehorn, N., Way, M., Wehland, J., and Rottner, K. (2002). Phosphatidylinositol 4,5-biphosphate (PIP2)-induced vesicle movement depends on N-WASP and involves Nck, WIP, and Grb2. J. Biol. Chem. *277*, 37771–37776.

Bishop, A.L., and Hall, A. (2000). Rho GTPases and their effector proteins. Biochem. J. *348*, 241–255.

Bompard, G., and Caron, E. (2004). Regulation of WASP/WAVE proteins: making a long story short. J. Cell Biol. *166*, 957–962.

Buck, M., Xu, W., and Rosen, M.K. (2001). Global disruption of the WASP autoinhibited structure on Cdc42 binding. Ligand displacement as a novel method for monitoring amide hydrogen exchange. Biochemistry *40*, 14115–14122.

Buck, M., Xu, W., and Rosen, M.K. (2004). A two-state allosteric model for autoinhibition rationalizes WASP signal integration and targeting. J. Mol. Biol. *338*, 271–285.

Carlier, M.F., Nioche, P., Broutin-L'Hermite, I., Boujemaa, R., Le Clainche, C., Egile, C., Garbay, C., Ducruix, A., Sansonetti, P., and Pantaloni, D. (2000). GRB2 links signaling to actin assembly by enhancing interaction of neural Wiskott-Aldrich syndrome protein (N-WASp) with actin-related protein (ARP2/3) complex. J. Biol. Chem. *275*, 21946–21952.

Cory, G.O.C., Cramer, R., Blanchoin, L., and Ridley, A.J. (2003). Phosphorylation of the WASP-VCA domain increases its affinity for the Arp2/3 complex and enhances actin polymerization by WASP. Mol. Cell *11*, 1229–1239.

Derry, J.M.J., Ochs, H.D., and Francke, U. (1994). Isolation of a novel gene mutated in Wiskott-Aldrich syndrome. Cell *78*, 635–644.

Devriendt, K., Kim, A.S., Mathijs, G., Frints, S.G., Schwartz, M., Van Den Oord, J.J., Verhoef, G.E., Boogaerts, M.A., Fryns, J.P., You, D., et al. (2001). Constitutively activating mutation in WASP causes X-linked severe congenital neutropenia. Nat. Genet. *27*, 313–317.

Dvorsky, R., and Ahmadian, M.R. (2004). Always look on the bright site of Rho: structural implications for a conserved intermolecular interface. EMBO Rep. *5*, 1130–1136.

Egile, C., Loisel, T.P., Laurent, V., Li, R., Pantaloni, D., Sansonetti, P.J., and Carlier, M.F. (1999). Activation of the CDC42 effector N-WASP by the Shigella flexneri IcsA protein promotes actin nucleation by Arp2/3 complex and bacterial actin-based motility. J. Cell Biol. *146*, 1319–1332.

Fiegen, D., Haeusler, L.C., Blumenstein, L., Herbrand, U., Dvorsky, R., Vetter, I.R., and Ahmadian, M.R. (2004). Alternative splicing of Rac1 generates Rac1b, a self-activating GTPase. J. Biol. Chem. *279*, 4743–4749.

Gizachew, D., Guo, W., Chohan, K.K., Sutcliffe, M.J., and Oswald, R.E. (2000). Structure of the complex of Cdc42Hs with a peptide derived from p-21 activated kinase. Biochemistry *39*, 3963–3971.

Higgs, H.N., and Pollard, T.D. (1999). Regulation of actin polymerization by Arp2/3 complex and WASp/Scar proteins. J. Biol. Chem. *274*, 32531–32534.

Higgs, H.N., and Pollard, T.D. (2000). Activation by Cdc42 and PIP2 of Wiskott-Aldrich syndrome protein (WASp) stimulates actin nucleation by Arp2/3 complex. J. Cell Biol. *150*, 1311–1320.

Ihara, K., Muraguchi, S., Kato, M., Shimizu, T., Shirakawa, M., Kuroda, S., Kaibuchi, K., and Hakoshima, T. (1998). Crystal structure of human RhoA in a dominantly active form complexed with a GTP analogue. J. Biol. Chem. *273*, 9656–9666.

Kiel, C., Selzer, T., Shaul, Y., Schreiber, G., and Herrmann, C. (2004). Electrostatically optimized Ras-binding Ral guanine dissociation stimulator mutants increase the rate of association by stabilizing the encounter complex. Proc. Natl. Acad. Sci. USA *101*, 9223–9228.

Kim, A.S., Kakalis, L.T., Abdul-Manan, M., Liu, G.A., and Rosen, M.K. (2000). Autoinhibition and activation mechanisms of the Wiskott-Aldrich syndrome protein. Nature *404*, 151–158.

Lapouge, K., Smith, S.J.M., Walker, P.A., Gamblin, S.J., Smerdon, S.J., and Rittinger, K. (2000). Structure of the TPR domain of p67(phox) in complex with Rac center dot GTP. Mol. Cell *6*, 899–907.

Miki, H., Miura, K., and Takenawa, T. (1996). N-WASP, a novel actin-depolymerizing protein, regulates the cortical cytoskeletal rearrangement in a PIP2-dependent manner downstream of tyrosine kinases. EMBO J. *15*, 5326–5335.

Miki, H., Sasaki, T., Takai, Y., and Takenawa, T. (1998). Induction of filopodium formation by a WASP-related actin-depolymerizing protein N-WASP. Nature *391*, 93–96.

Miki, H., and Takenawa, T. (2003). Regulation of actin dynamics by WASP family proteins. J. Biochem. (Tokyo) *134*, 309–313.

Millard, T.H., Sharp, S.J., and Machesky, L.M. (2004). Signalling to actin assembly via the WASP (Wiskott-Aldrich syndrome protein)-family proteins and the Arp2/3 complex. Biochem. J. *380*, 1–17.

Neudauer, C.L., Joberty, G., Tatsis, N., and Macara, I.G. (1998). Distinct cellular effects and interactions of the Rho-family GTPase TC10. Curr. Biol. *8*, 1151–1160.

Owen, D., Mott, H.R., Laue, E.D., and Lowe, P.N. (2000). Residues in Cdc42 that specify binding to individual CRIB effector proteins. Biochemistry *39*, 1243–1250.

Pantaloni, D., Boujemaa, R., Didry, D., Gounon, P., and Carlier, M.F. (2000). The Arp2/3 complex branches filament barbed ends: functional antagonism with capping proteins. Nat. Cell Biol. *2*, 385–391.

Passey, S., Pellegrin, S., and Mellor, H. (2004). What is in a filopodium? Starfish versus hedgehogs. Biochem. Soc. Trans. *32*, 1115–1117.

Peterson, J.R., Bickford, L.C., Morgan, D., Kim, A.S., Ouerfelli, O., Kirschner, M.W., and Rosen, M.K. (2004). Chemical inhibition of N-WASP by stabilization of a native autoinhibited conformation. Nat. Struct. Mol. Biol. *11*, 747–755.

Prehoda, K.E., Scott, J.A., Mullins, R.D., and Lim, W.A. (2000). Integration of multiple signals through cooperative regulation of the N-WASP-Arp2/3 complex. Science *290*, 801–806.

Rohatgi, R., Ho, H.Y.H., and Kirschner, M.W. (2000). Mechanism of N-WASP activation by CDC42 and phosphatidylinositol 4,5-bisphosphate. J. Cell Biol. *150*, 1299–1309.

Rohatgi, R., Ma, L., Miki, H., Lopez, M., Kirchhausen, T., Takenawa, T., and Kirschner, M.W. (1999). The interaction between N-WASP and the Arp2/3 complex links Cdc42-dependent signals to actin assembly. Cell *97*, 221–231.

Rudolph, M.G., Bayer, P., Abo, A., Kuhlmann, J., Vetter, I.R., and Wittinghofer, A. (1998). The Cdc42/Rac interactive binding region motif of the Wiskott-Aldrich syndrome protein (WASP) is necessary but not sufficient for tight binding to Cdc42 and structure formation. J. Biol. Chem. *273*, 18067–18076.

Schreiber, G. (2002). Kinetic studies of protein-protein interactions. Curr. Opin. Struct. Biol. *12*, 41–47.

Sheinerman, F.B., Norel, R., and Honig, B. (2000). Electrostatic aspects of protein-protein interactions. Curr. Opin. Struct. Biol. *10*, 153–159.

Sinha, N., and Smith-Gill, S.J. (2002). Electrostatics in protein binding and function. Curr. Protein Pept. Sci. *3*, 601–614.

Suetsugu, S., Hattori, M., Miki, H., Tezuka, T., Yamamoto, T., Miko-

shiba, K., and Takenawa, T. (2002). Sustained activation of N-WASP through phosphorylation is essential for neurite extension. Dev. Cell *3*, 645–658.

Symons, M., Derry, J.M.J., Karlak, B., Jiang, S., Lemahieu, V., McCormick, F., Francke, U., and Abo, A. (1996). Wiskott-Aldrich syndrome protein, a novel effector for the GTPase CDC42Hs, is implicated in actin polymerization. Cell *84*, 723–734.

Takenawa, T., and Miki, H. (2001). WASP and WAVE family proteins: key molecules for rapid rearrangement of cortical actin filaments and cell movement. J. Cell Sci. *114*, 1801–1809.

Thrasher, A.J. (2002). WASp in immune-system organization and function. Nat. Rev. Immunol. *2*, 635–646.

Torres, E., and Rosen, M.K. (2003). Contingent phosphorylation/dephosphorylation provides a mechanism of molecular memory in WASP. Mol. Cell *11*, 1215–1227.

Vignal, E., De Toledo, M., Comunale, F., Ladopoulou, A., Gauthier-Rouviere, C., Blangy, A., and Fort, P. (2000). Characterization of TCL, a new GTPase of the Rho family related to TC10 and Cdc42. J. Biol. Chem. *275*, 36457–36464.

Yang, C.S., Huang, M.Z., DeBiasio, J., Pring, M., Joyce, M., Miki, H., Takenawa, T., and Zigmond, S.H. (2000). Profilin enhances Cdc42-induced nucleation of actin polymerization. J. Cell Biol. *150*, 1001–1012.

Accession Numbers

The coordinates of human TC10·GppNHp have been deposited in the Protein Data Bank under accession code 2ATX.